International Journal of Biological Macromolecules 121 (2019) 699–706

Contents lists available at ScienceDirect

International Journal of Biological Macromolecules

journal homepage: http://www.elsevier.com/locate/ijbiomac

A novel GelMA-pHEMA hydrogel nerve guide for the treatment of peripheral nerve damages

Tugba Dursun Usal [a,b,c], Deniz Yucel [a,d], Vasif Hasirci [a,b,c,d,*]

[a] Middle East Technical University (METU), BIOMATEN, Center of Excellence in Biomaterials and Tissue Engineering, Ankara, Turkey
[b] METU, Department of Biotechnology, Ankara, Turkey
[c] METU, Department of Biological Sciences, Ankara, Turkey
[d] Acıbadem Mehmet Ali Aydinlar University, School of Medicine, Department of Histology and Embryology, Istanbul, Turkey

ARTICLE INFO

Article history:
Received 29 August 2018
Received in revised form 8 October 2018
Accepted 14 October 2018
Available online 15 October 2018

ABSTRACT

Damage to the nervous system due to age, diseases or trauma may inhibit signal transfer along the nervous system. Nerve guides are used to treat these injuries by bridging the proximal and the distal end together. The design of the guide is very important for the reconnection of the severed axons. Methacrylated gelatin-poly(2-hydroxyethylmethacrylate) (GelMA-pHEMA) hydrogel was produced as the outer part of the nerve guide. pHEMA was added in various amounts into GelMA and increased the mechanical strength which is needed for the suturability of the guide. Porosity (15–70%), pore size (10–35 μm), water content (42–92%), and mechanical strength (65–710 kPa) of GelMA-pHEMA hydrogels were found to be suitable for nerve tissue engineering applications. Schwann cells attached and proliferated on GelMA, GelMA-pHEMA (5:5), and pHEMA hydrogels. Providing guidance is very important in the development of a nerve guide due to the anisotropic nature of the nerve tissue. Therefore, gelatin-poly(3-hydroxybutyrate-*co*-3-hydroxyvalerate) (PHBV) aligned fiber mats were used inside of the nerve guide. High degree of alignment with low deviation (7°) of this mats provided PC12 cell alignment throughout the fibers. Combination of GelMA-pHEMA (5:5) hydrogel and gelatin-PHBV aligned mat would provide an ideal nerve guide for the treatment of peripheral nerve damages.

1. Introduction

When the peripheral nervous system (PNS) is injured, the axons are capable of regenerating only short defect segments (<2 mm). However, the regenerating axon may stay disconnected and full function may not be recovered [1]. Nerve tissue undergoes three main processes to achieve full recovery: Wallerian degeneration, axonal regeneration, and end-organ reinnervation [2]. During nerve recovery, the axonal outgrowth becomes remyelinated by the resident Schwann cells [3]. Peripheral crush injuries cause different degrees of neural damage [4]. They occur from an acute traumatic compression of the nerve from a blunt object such as surgical clamp and do not result in a complete transection of the nerve. There are different strategies to treat these damages. End to end suturing of the damaged nerve is used when the gap is small. From the tissue engineering perspective, nerve guides are produced to provide peripheral nerve regeneration at the crushed site. The novel strategies are developing advanced microarchitecture such as aligned fibers to provide an alignment, controlled release of neural growth factors to enhance regeneration, using supportive cells such as Schwann cells or stem cells to remyelinate the axons, and mimicking natural extracellular matrix (ECM) of the peripheral nerves [5].

Synthetic polymers such as silicone [6], poly(2-hydroxyethylmethacrylate) (pHEMA) [7], polyethylene glycol (PEG) [8,25], and polypyrole (PPy) [9] are used to produce nerve guides. However, most of them are hydrophobic and nondegradable which make them not suitable for the nerve tissue engineering purposes. Natural polymers such as collagen [10], gelatin [11], chitosan [12], hyaluronic acid [13] and silk fibroin [14] are also used to fabricate nerve guides [15]. Although they are biodegradable and biocompatible, they often lack the mechanical strength which is needed for the suturability of the nerve guide at the injured site. Making a blend of these polymers could create the ideal nerve guide for peripheral nerve crush injuries. Nerve tissue is considered as a soft tissue, because Young's Modulus of a rat sciatic nerve is very low (580 ± 150 kPa) [16,17]. Hydrogels are suitable for a variety of tissue engineering applications because they carry large amounts of water. This property makes them soft and rubbery which resemble living tissues. Therefore, it is easier to mimic nerve tissue by using a hydrogel based nerve guide. In this study, a natural polymer gelatin was methacrylated (GelMA) and combined with a synthetic polymer poly(2-hydroxyethylmethacrylate) to increase its mechanical strength to construct the outer part of the nerve guide which was seeded with Schwann cells as the support cells. Schwann

* Corresponding author at: Acıbadem Mehmet Ali Aydinlar University, School of Medicine, Department of Histology and Embryology, Istanbul, Turkey.
E-mail address: vhasirci@acibadem.edu.tr (V. Hasirci).

https://doi.org/10.1016/j.ijbiomac.2018.10.060
0141-8130/

cells form regeneration tracks in the distal stump which provides guidance of the regenerating axons to their targets and they also provide essential trophic support for injured neurons [18]. Therefore, Schwann cells (SCs) are incorporated in the structure of the nerve guides in many applications [19,20]. In 2016, autologous Schwann cells were combined with sural nerve grafts for the first time to repair a human large sciatic nerve defect (7.5 cm) after a traumatic nerve injury [21]. Patient had proximal sensory recovery, motor recovery, and improvement in her pain scores over time. PC12 cells (pheochromocytoma cells) are derived from the adrenal gland of *Rattus norvegicus*, and were used as an in vitro model system for nerve regeneration as it is the much frequently used in vitro studies involving neurite outgrowth. Furthermore, primary cell cultures are not immortal, therefore, the number of cells available for experiments is very low [22].

Electrospun fibers are used in regenerative medicine because nanofibrous structures developed by electrospinning technology carry some of the properties of the extracellular matrix suitable for the anchorage, migration, and differentiation of cells [23]. Nano and micro fibers have large surface area-to-volume ratio, high porosity, and easily processed into a variety of sizes and shapes, and their composition can be modified to match the properties and functionality of the desired tissue engineering products. Aligned fibrous mats are usually preferred in the composition of a nerve guide to provide the anisotropic nerve tissue formation [24]. Extensive studies put a remark on the importance of the alignment in the nerve guides [19,26,21,27]. Gelatin and poly(3-hydroxybutyrate-*co*-3-hydroxyvalerate) (PHBV) were blended and electrospun together to obtain the inner part of the nerve guide. Both PHBV, a biopolymer, and gelatin, another natural polymer, with different rates of degradability were used to form a sacrificial fibrous system [28]. One problem about using fibrous mats is that they are too crowded and do not allow the migration of the cells properly. However, cells can have space to migrate when a sacrificial fibrous system is achieved. Gelatin has faster degradation than the PHBV, therefore, nerve cells can have more space as the incubation continues.

In this study, GelMA-pHEMA hydrogel nerve guide seeded with the Schwann cells was prepared for the first time to treat peripheral nerve crushes as the outer part of the nerve guide. Aligned gelatin-PHBV fiber mats were produced by electrospinning to provide guidance of the nerve cells inside of the nerve guide. An in vitro testing of this composite nerve guide was achieved successfully and a suturable nerve guide was obtained.

2. Materials and methods

2.1. Materials

Hydroxyethyl methacrylate (HEMA) monomer, ethyleneglycol dimethacrylate (EGDMA), poly(3-hydroxybutyrate-*co*-3-hydroxyvalerate) (PHBV5), type A porcine skin gelatin (70–100 bloom), 2-(Hydroxyl)-4-(2-hydroxyethoxy)-2-methylpropiophenone (Irgacure 2959), methacrylic anhydride, 1,1,1,3,3,3-hexafluoroisopropanol (HFIP), bovine serum albumin (BSA), FITC-labeled phalloidin, DRAQ5, NGF-β from rat and Alexafluor532-conjugated anti-mouse Ig antibody were purchased from Sigma (USA and Germany). DMEM-High glucose, DMEM-High glucose colorless, fetal bovine serum (FBS), trypsin-EDTA were purchased from Thermo Scientific (USA). Ammonium persulfate (APS), dimethyl sulfoxide (DMSO), and Triton-X 100 were obtained from AppliChem (Germany).

2.2. Synthesis of methacrylated gelatin (GelMA)

Methacrylated gelatin was synthesized according to literature [29]. Type A porcine skin gelatin (Sigma, USA) was mixed with PBS to form a 10% (w/v) solution at 60 °C and stirred until completely dissolved. Methacrylic anhydride (MA) (94%, Sigma, USA) was added into this solution to create a 20% (v/v) solution. It was diluted 5× with warm (40 °C) PBS after 1 h reaction at 50 °C, and the final solution was dialyzed in a dialysis tubing (CO 10000) against distilled water for 1 week at 40 °C to remove excess methacrylic acid. It is lyophilized for 1 week until a white porous foam was obtained.

2.3. Determination of methacrylic acid content of GelMA with NMR

Gelatin and GelMA polymers were dissolved in D_2O at 30 mg/mL at 40 °C. ^1H NMR spectra were obtained at room temperature (RT) on a Bruker DPX 400 spectrometer operating at a ^1H resonance frequency of 400 MHz and sixteen scans were acquired for signal-to-noise averaging.

2.4. Preparation of GelMA-pHEMA hydrogels

GelMA (15%, w/v) in PBS carrying 0.5% photoinitiator (Irgacure 2959) (w/v) were poured into PDMS molds and exposed to UV (365 nm, 0.120 J/cm^2) for 1 min in a UV crosslinker chamber (BIO-LINKTM UV Crosslinker DLX-365, Germany). The final product had pHEMA in various proportions (9:1, 8:2, 7:3, 6:4, 5:5, v/v) to obtain an optimum hydrogel formation.

2.5. FTIR analysis

Gelatin, uncrosslinked GelMA and crosslinked GelMA surfaces were analyzed with FTIR-ATR spectroscopy (Perkin Elmer Spectrum, Frontier, Massachusetts, USA) to show the methacrylation of the gelatin. All samples were scanned 4 times in the range 400–4000 cm^{-1} with a resolution of 4 cm^{-1}.

2.6. SEM and ImageJ analysis

Scaffolds were coated with gold-palladium (Au—Pd) under vacuum and examined with SEM (Quanta 400F Field Emission SEM, Netherlands). Surface and the cross-section porosity and pore size of GelMA-pHEMA hydrogels were determined with ImageJ (NIH, USA) analysis.

2.7. Water content determination

The water content of hydrogels was determined by measuring the changes in their weights upon water absorption. Samples were incubated at 37 °C for 12 h in a water bath, wiped with filter paper to remove the excess water and weighed. Water Content (WC) was calculated according to the following equation:

$$WC\ (\%) = ((W_w - W_d)/W_w) \times 100 \quad (1)$$

where W_w is the weight of wet samples, and W_d is the weight of dry samples.

2.8. Degradation test in PBS

Scaffolds were weighed to a sensitivity of 0.1 mg and incubated in PBS (10 mM, pH 7.4) at 37 °C for 4 weeks to study the degradation behavior in PBS. The samples were removed from PBS, rinsed with distilled water 3 times, lyophilized and weighed. Weight loss was determined weekly for 4 weeks ($n = 3$). The extent of degradation was determined gravimetrically as the percent weight loss according to following equation:

$$\text{Remaining weight}\ (\%) = ((W_0 - W_d)/W_d) \times 100 \quad (2)$$

where Wo is the original dry weight and Wd is the dry weight after incubation.

2.9. Mechanical tests

Tensile mechanical tests were conducted on a Shimadzu AGS-X Universal Testing Machine (Japan) at a displacement rate of 2 mm/min at RT. The pHEMA and GelMA-pHEMA hydrogels were brought to equilibrium swelling in distilled water (24 h, RT) and rectangular test samples (30 mm × 10 mm) were cut and tensile modulus of the scaffolds was calculated. Compression tests were conducted on a Univert, CellScale mechanical test system (Canada) at a displacement rate of 1 mm/min in vertical direction and compressive modulus of the scaffolds was calculated. Stress (σ), strain (ε), tensile and compressive modulus of the samples were calculated as in Eqs. (3), (4), and (5).

$$\text{Stress } (\sigma) = F/A \tag{3}$$

$$\text{Strain } (\varepsilon) = \Delta l/l \tag{4}$$

$$\text{Tensile/Compressive modulus} = \sigma/\varepsilon \tag{5}$$

where F is the applied force, A is the cross-sectional area, l is sample length, and Δl is the displacement.

2.10. Preparation of gelatin-PHBV fiber mats

Gelatin-PHBV solutions (5, 10, 15, %, w/v) were prepared in HFIP. The solutions were prepared and transferred into a syringe. Positive pole of the power supply was connected to the metal syringe tip, and the negative pole was connected to the copper ground of the collector. To obtain aligned fibers, a copper plate with parallel grids was used as the collector as was previously described [30]. 11 kV potential was applied. Distance between the syringe needle and the collector was 11 cm, and flow rate was 4 μL/min.

2.11. In vitro studies

2.11.1. Schwann cell seeding on GelMA-pHEMA hydrogels

Mouse neuronal Schwann cells (ATCC CRL-2766) were seeded on the GelMA, GelMA-pHEMA (5:5), and pHEMA hydrogels. Cells were grown in DMEM high glucose tissue culture medium containing penicillin (100 U/mL), streptomycin (100 μg/mL), and 10% FBS. Aliquots of the cell suspension were seeded on scaffolds to achieve a cell density of 1 × 10^5 cells/cm^2. The cell seeded hydrogels were incubated at 37 °C and 5% CO_2 for 2 h to ensure attachment of the cells. Then, fresh medium was added onto the hydrogels, and incubation continued for three weeks with the medium being refreshed every 2 days.

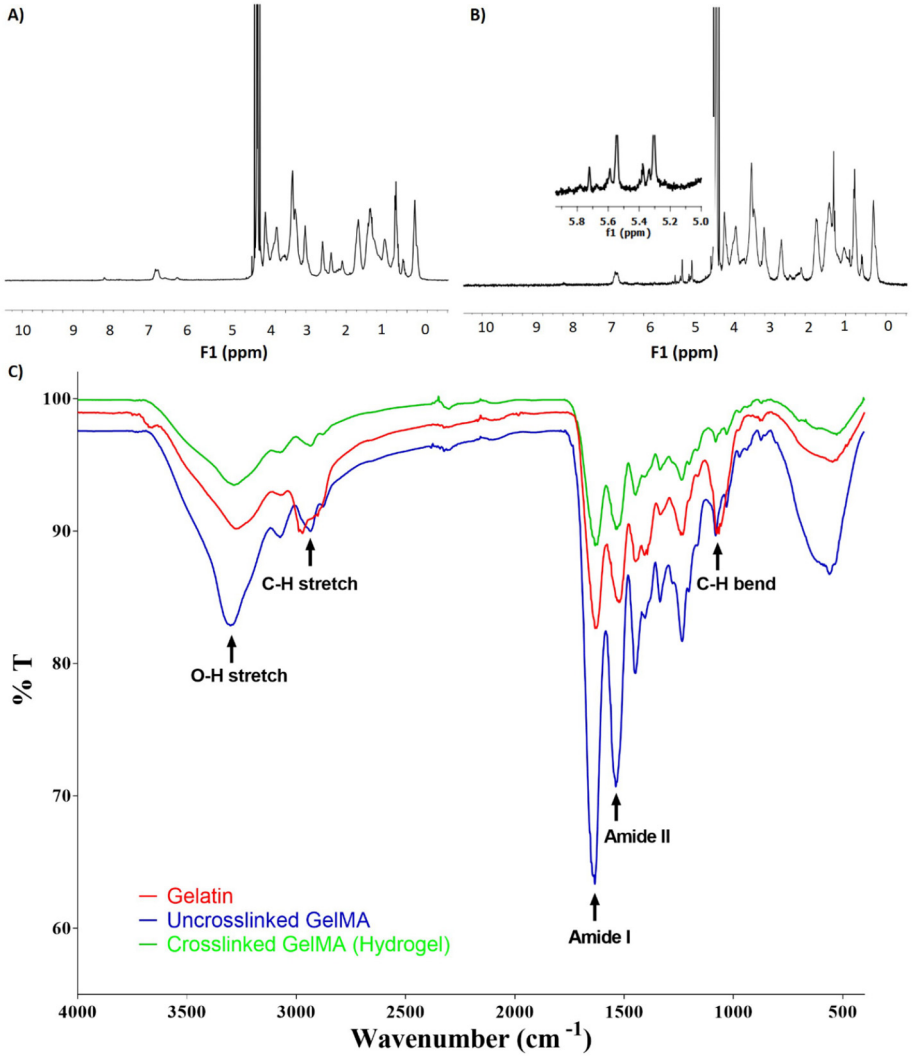

Fig. 1. Characteristics of gelatin, uncrosslinked GelMA, and crosslinked GelMA. ^{1}H NMR spectra of A) Gelatin and B) Methacrylated gelatin (GelMA), C) FTIR spectra of gelatin, uncrosslinked and crosslinked GelMA.

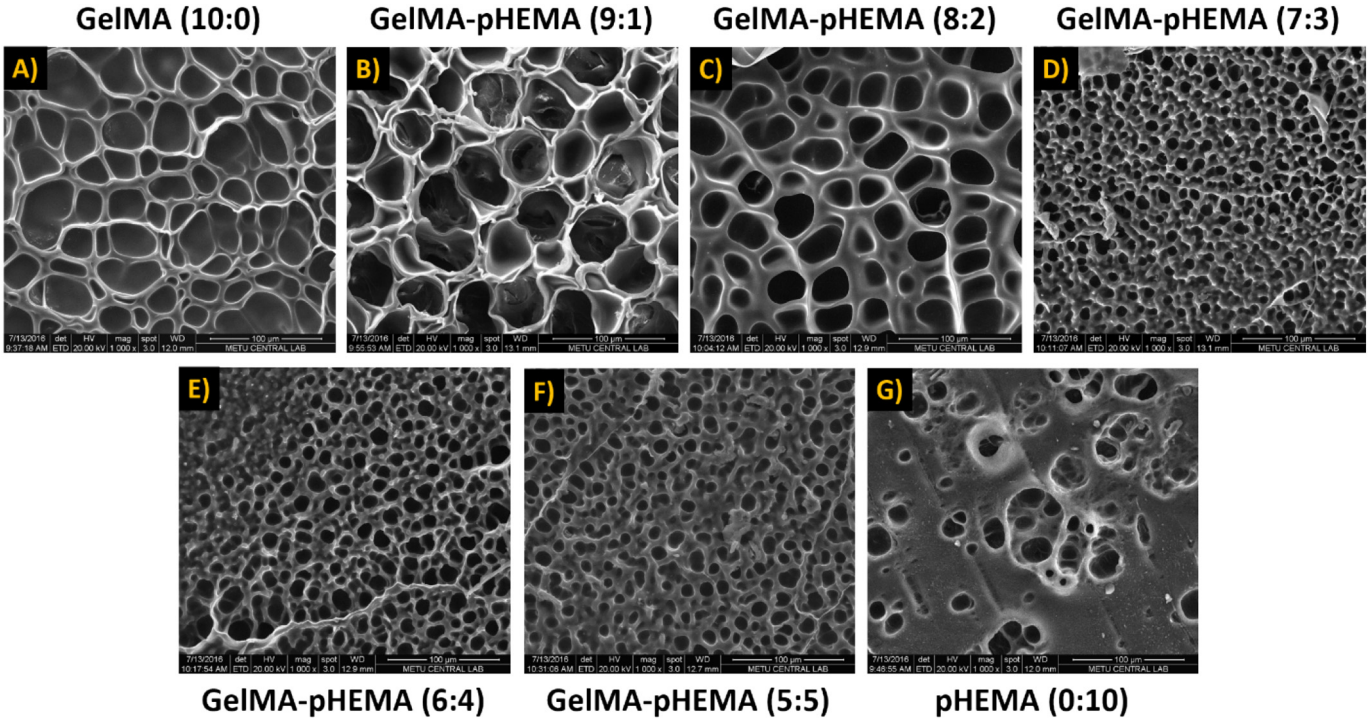

Fig. 2. SEM micrographs of surface of A) GelMA, B) GelMA-pHEMA (9:1), C) GelMA-pHEMA (8:2), D) GelMA-pHEMA (7:3), E) GelMA-pHEMA (6:4), F) GelMA-pHEMA (5:5), G) pHEMA hydrogels. 1000×.

2.11.2. PC12 cell seeding on aligned gelatin-PHBV mats

PC12 cells (pheochromocytoma cells derived from the adrenal gland of *Rattus norvegicus*) (ATCC CRL-1721.Adh) were grown in Ham's F12 tissue culture medium containing penicillin (100 U/mL), streptomycin (100 μg/mL), 2.5% FBS, and 15% horse serum, 50 ng/mL NGF. Aliquots of the cell suspension were seeded on 15% gelatin-PHBV aligned fibers to achieve a cell density of 5×10^5 cells/cm^2. The cell seeded fibrous mats were incubated at 37 °C and 5% CO_2 for 2 h to ensure attachment of the cells. Then, fresh medium was added onto the scaffolds, and incubation continued for three weeks with the medium being refreshed every 2 days.

2.11.3. Cell attachment and proliferation

Alamar Blue Cell Viability Assay was performed to quantify the cell attachment and proliferation on the hydrogels. Alamar Blue is a water

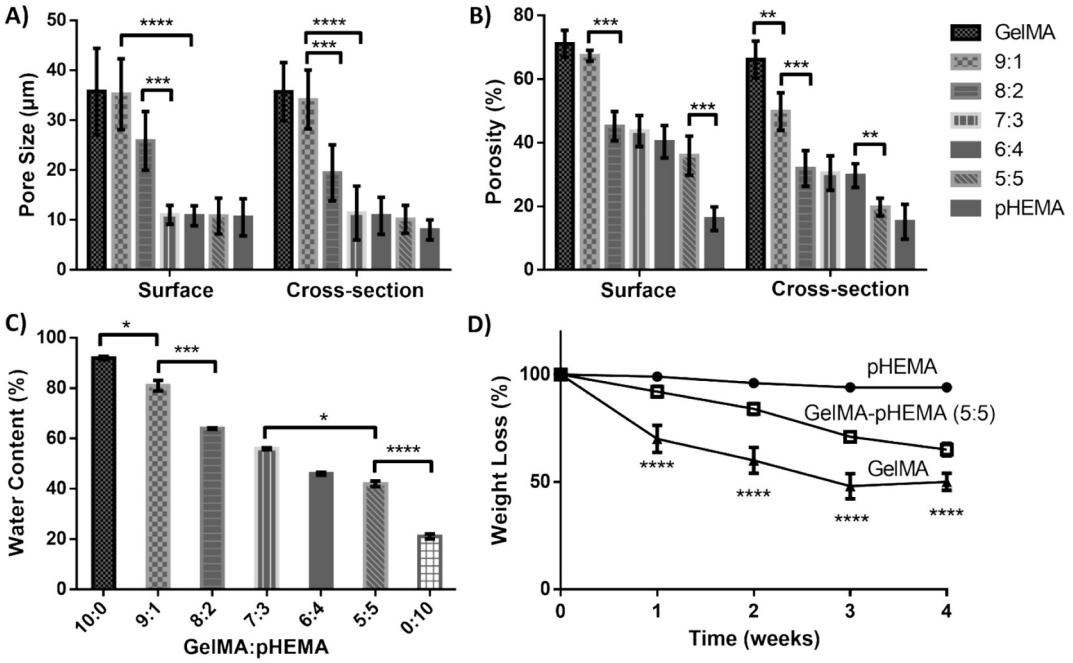

Fig. 3. Characterization of the GelMA-pHEMA the hydrogels. A) Porosity of the hydrogels, B) Pore size of hydrogels (ImageJ), C) Water content of the hydrogels, D) Weight loss of the hydrogels over 4 weeks. Statistical differences (*p ≤ 0.05, **p ≤ 0.01, ***p ≤ 0.001, ****p ≤ 0.0001) are indicated.

Table 1
Mechanical characteristics of GelMA, GelMA-pHEMA (5:5), pHEMA hydrogels.

Samples	Tensile modulus (kPa)	Ultimate tensile strength (kPa)	Compressive modulus (kPa)
pHEMA	710 ± 150	200 ± 70	163 ± 29
GelMA-pHEMA (5:5)	320 ± 60	140 ± 50	65 ± 10
GelMA	–	–	1.73 ± 0.15

Table 2
Characteristics of Gelatin-PHBV fiber mats.

Concentration of gelatin-PHBV solution in HFIP (%, w/v)	Degree of alignment (°)	Porosity (%)	Fiber diameter (μm)
5	46	44 ± 3	0.3 ± 0.2
10	21	51 ± 2	1.2 ± 0.5
15	7	44 ± 3	3.2 ± 2.1

soluble dye in the oxidized form and is reduced in the cytosol by mitochondrial enzyme activity of the live cells by accepting electrons from NADPH, FADH, and NADH [31]. This redox reaction results in the colour of the culture medium to change from Indigo Blue (resazurin) to fluorescent pink (resorufin). The UV–Vis absorbances or fluorescence intensity are measured with a UV–Vis spectrophotometer or a spectrofluorimeter at 570 and 595 nm. Reductions were calculated according to the protocol of the producer (Invitrogen Inc., USA).

2.11.4. Confocal laser scanning microscopy

The growth medium of the cell-seeded GelMA-pHEMA hydrogels and gelatin-PHBV mats was discarded, and cells were fixed with 4% (w/v) paraformaldehyde at RT for 15 min. Cell membrane was permeabilized with Triton X-100 (1% v/v in PBS pH 7.4) at RT for 5 min. After washing, samples were incubated in BSA (1% w/v in PBS) at 37 °C for 30 min. Alexa Fluor® 488-Phalloidin (1:200 w/v, prepared in 0.1% BSA, w/v in PBS), was added to the samples and stored at RT for 1 h to stain the actin filaments of the cytoskeleton. After two washes with PBS, samples were incubated with DRAQ5 (Sigma, USA) for 30 min at RT to stain the cell nuclei. Samples were washed twice with PBS and stored in PBS solution until examination using a Confocal Laser Scanning Microscope (Leica, Germany).

2.12. Statistical analysis

Statistical analyses were performed using a two-way analysis of variance (ANOVA) with Tukey's post hoc test or Student's *t*-test with a minimum confidence level of 95%, p values smaller or equal to 0.05 were considered statistically significant. All values were reported as the mean ± standard deviation.

3. Results and discussion

3.1. Methacrylic acid (MA) content of GelMA

Methacrylation of gelatin was verified using H^1 NMR. Degree of methacrylation (DM) is defined as the number of methacrylated groups attached to gelatin divided by the number of amine groups on pristine native gelatin [32]. DM was calculated by dividing the integrated peaks at 5.3 ppm and 5.5 ppm due to double bond hydrogens of methacrylate groups to integrated peaks at 7.2 ppm due to aromatic residues of gelatin [29]. NMR results showed 65% DM in this study. Fig. 1 shows the NMR spectra of gelatin and methacrylated gelatin. 5.3 ppm and 5.5 ppm peaks are absent on the spectrum of gelatin verifying that there are no double bonds on native gelatin.

3.2. FTIR characterization

The FTIR spectrum of gelatin, uncrosslinked GelMA and crosslinked GelMA shows the following relevant bands (Fig. 1C): 3300 cm^{-1} (O—H stretching vibrations), 2922 cm^{-1} (C—H stretching), 1640 cm^{-1} (O—H bonding), and 1525 cm^{-1} (C—N stretching and N—H bending) [33]. There was a decrease in the peak around 3300 cm^{-1} related to the decrease in the total number of –OH groups in the structure due to UV crosslinking [34]. Also, it is possible to verify the decrease of the peak related to the C—C bond at 3010 cm^{-1}, suggesting the success of the photopolymerization and the consequent introduction of GelMA in the final structure of the hydrogel [35]. The typical amide I and II bands at 1640 cm^{-1} and 1540 cm^{-1} (due to C═O stretching and N—H bending respectively) are present in all of the materials, however their intensities are different from each other. When the gelatin and GelMA spectra compared, there are differences in the C—H stretching and bending areas due to the addition of the methacrylate groups into the lysine groups of gelatin.

3.3. SEM and degradation of hydrogels

Interconnected porous structures provide a good environment for cell ingrowth, vascularization, and nutrient diffusion, which are critical for cell survival. Porosity, pore size distribution and the average pore dimension of scaffolds are very important in cell migration, nutrient penetration, and waste removal [36]. SEM micrographs of GelMA, GelMA-pHEMA blends (9:1, 8:2, 7:3, 6:4, 5:5), and pHEMA hydrogel surface were shown on Fig. 2. As the amount of pHEMA increases, porosity, pore size and water content of the hydrogels decreases significantly. This is also confirmed by ImageJ analysis which is used for porosity and pore size calculation of the hydrogels (Fig. 3). While GelMA has the highest porosity (70%), pHEMA has the lowest (15%). Blends of these two (9:1, 8:2, 7:3, 6:4, 5:5) have the porosity between these values (20–65%). This phenomenon is also same for pore size (15–40 μm).

In tissue engineering, biodegradable scaffolds are preferred because in the tissue reconstruction process initially the cells are grown on the

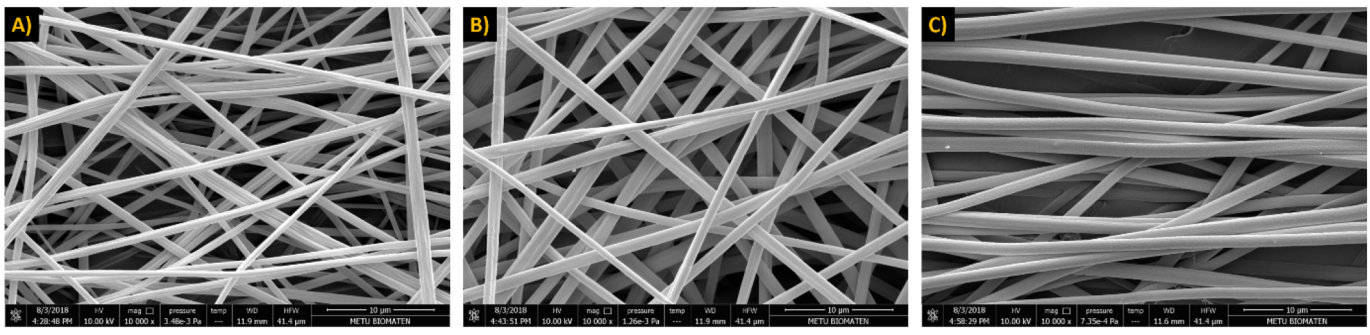

Fig. 4. SEM micrographs of Gelatin-PHBV fiber mats. A) 5%, B) 10%, and C) 15% polymer concentration. 10,000×.

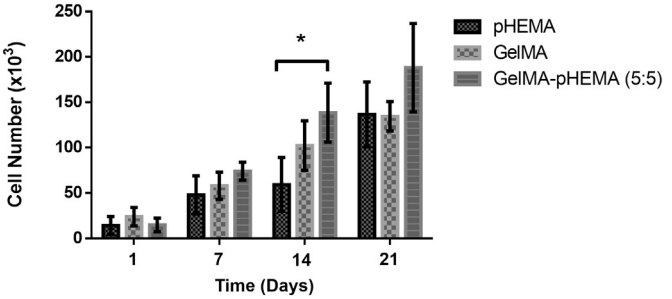

Fig. 5. Schwann cell proliferation on pHEMA, GelMA and GelMA-pHEMA (5:5) hydrogels over 3 weeks. Initial cell seeding density: 10^5 cells/cm^2. Statistical differences (*p ≤ 0.05) are indicated.

scaffolds, then they penetrate the structure and in the meantime, the scaffold degrades creating more space for cell growth [37]. Meanwhile, cells deposit new extracellular matrix (ECM) that replaces the scaffold. In the end, the scaffold is expected to completely disappear. ECM deposition rate should match the scaffold degradation rate for proper healing. Thus, the degradation time should be optimized according to the tissue targeted. Weight loss of GelMA, GelMA-pHEMA (5:5), and pHEMA hydrogels are presented in Fig. 3D. Degradation of pHEMA was much slower than the GelMA and GelMA-pHEMA (5:5). Fastest degradation occurred with the GelMA hydrogels which lose half of its content over four weeks. However, this degradation rate is suitable for cell growth. As it is stated in the above, degradation provides more space for cell growth.

3.4. Mechanical tests

Tensile mechanical tests were applied to only pHEMA and GelMA-pHEMA (5:5) blend because other blend hydrogels (9:1, 8:2, 7:3, 6:4) were very soft, therefore, could not withstand the pressure during tension. Tensile modulus and the ultimate tensile strength (UTS) of the pHEMA and GelMA-pHEMA (5:5) hydrogels are given at Table 1. Compressive modulus of pHEMA is higher than that of GelMA-pHEMA (5:5) and GelMA hydrogels. It is observed that both tensile and compression values of GelMA-pHEMA (5:5) hydrogel are almost half of those pHEMA. These results reveal that pHEMA successfully increased the mechanical strength of the nerve guide.

In a study by Borschel et al. (2003), UTS and tensile modulus of a rat sciatic nerve tissue were found to be 2720 kPa and 580 kPa, respectively. Decellularized nerve tissue was reported to have a UTS of 1400 kPa and an elastic modulus of 576 kPa [17]. Although the UTS of pHEMA and GelMA-pHEMA are lower than the values of rat sciatic nerve tissue and decellularized nerve tissue, tensile modulus of the GelMA-pHEMA (5:5) is close to the values of those. Besides upon cell growth, the mechanical strength is expected to increase significantly due to the secretion of extracellular matrix proteins [38]. Tensile modulus of pHEMA hydrogel is even higher than decellurized nerve tissue. Therefore, both GelMA-pHEMA (5:5) and pHEMA hydrogel could serve as the outer part of a nerve guide.

3.5. Characterization of the gelatin-PHBV fiber mats

Two types of polymers with different degradation rates, gelatin and PHBV, were used to construct a sacrificial fiber system. Gelatin has faster degradation than PHBV, therefore, it could create more space for the cell

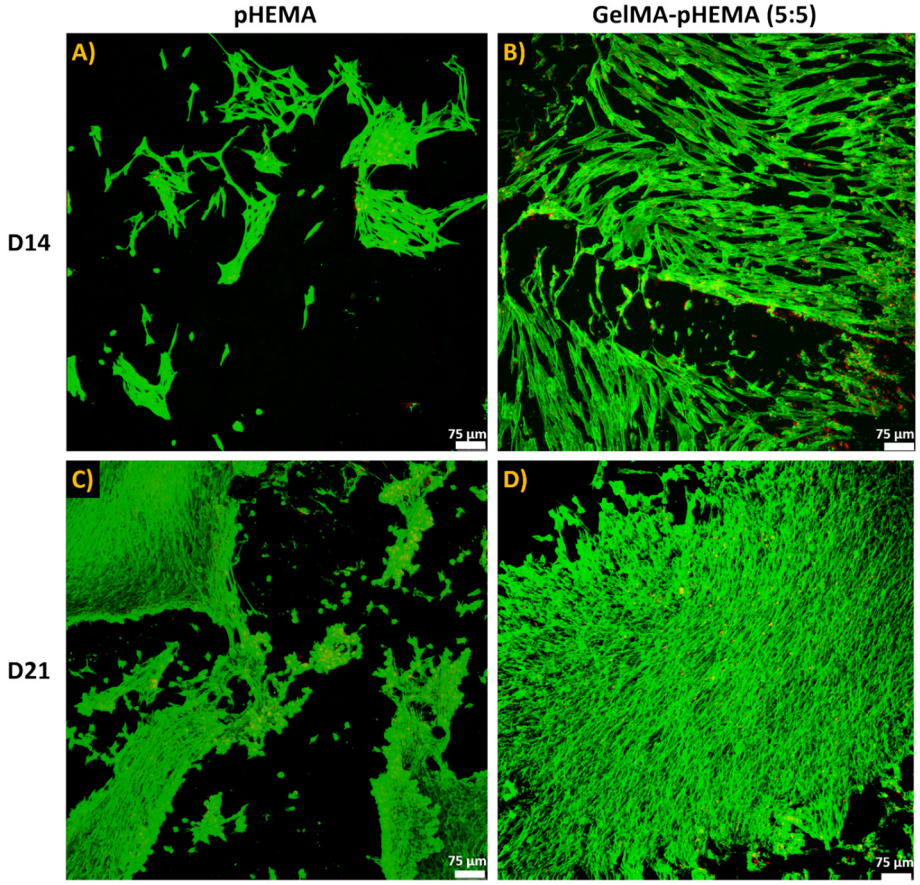

Fig. 6. Cytoskeleton (green) and nucleus (red) merged CLSM images of Schwann cells on A) pHEMA, D14 B) GelMA-pHEMA (5:5), D14 C) pHEMA, D21 D) GelMA-pHEMA (5:5), D21.

growth as it degrades. Overcrowding of the fibers which is a problem for the cell growth and migration is prevented by using this sacrificial system. Alignment is also very significant for a nerve guide because cells need topographical cues for their migration. It is critical to align the nerve cells inside of the nerve guide to provide successful nerve regeneration at the damaged area because nerve tissue is anisotropic. Different polymer concentrations (5, 10, 15, %, w/v) are prepared to obtain the highest degree of alignment (Fig. 4). As the polymer concentration increased, degree of alignment also increased. Using NIH, ImageJ program it was found that the highest degree of alignment with low deviation (7°) was achieved with 15% polymer concentration (Table 2). Fiber diameter of the 15% polymer concentration is in the range of 1–5 μm which is suitable for cell attachment and growth [39].

3.6. Schwann cell proliferation on hydrogels

The proliferation of Schwann cells seeded on GelMA, GelMA-pHEMA (5:5) and pHEMA hydrogels was studied with Alamar Blue assay (Fig. 5). Cell attachment was successful and Schwann cells proliferated very well on all hydrogel surfaces; cell numbers increased significantly as the culture duration increased. On Day 14, Schwann cell proliferation was higher on GelMA, GelMA-pHEMA (5:5) hydrogels than on pHEMA, but all supported Schwann cell growth indicating that any of them could be used as a nerve guide material in the treatment of peripheral nerve crush injuries.

3.7. Confocal microscopy

CLSM studies were carried out to study the cell material interaction. Alexa Fluor® 488-Phalloidin was used to stain the cytoskeleton (green) and DRAQ5 to stain the nuclei (red) of SCs. Fig. 6 shows the Schwann cell (SC) proliferation on GelMA-pHEMA (5:5) and pHEMA hydrogels. On Day 14, cell-to-cell interactions were apparent. More cells attached on GelMA-pHEMA (5:5) hydrogel probably due to the cell attractive properties of gelatin. On Day 21, the surface of hydrogels was covered with cells which formed a network. All type of hydrogels (GelMA, GelMA-pHEMA (5:5), pHEMA) were suitable for Schwann cell proliferation.

PC12 cells seeded on gelatin-PHBV (5:5) aligned fibrous mats are presented in Fig. 7. At the beginning, cells were aligned throughout the fibers and continued to grow on these surfaces over the time. On Day 7, cell-to-cell interaction became more apparent. At the end of the incubation (Day 21), all of the mats surface was covered with PC12 cells. It can be concluded that, this gelatin-PHBV mat surface is an excellent surface for cell attachment and proliferation. Using of this surface on the nerve guide inner part would make the nerve guide very attractive for the attachment and alignment of the damaged neurons at the injured site. Disconnected neurons can easily find each other throughout the gelatin-PHBV aligned fibrous mats. It can be said that PC12 cells appear to have penetrated into these mats and fully populated in them by examining z-section of these mats. As the incubation duration increased, cell penetration is also increased.

4. Conclusions

In this study, it was aimed to produce a hydrogel based, composite nerve guide which includes fibrous inner guidance elements produced by electrospinning. For this purpose, components of nerve guide structure, GelMA, pHEMA hydrogels as the outer part and 15% gelatin-PHBV fibrous mats as the inner part of the nerve guide with optimal properties (e.g. porosity, pore size, degradability) were tested in situ and in vitro for their suitability for use in the treatment of peripheral nerve crushes. It was found that their properties such as porosity, pore size, degradation, mechanical strength and degree of alignment were suitable. Among the different types of blends, GelMA-pHEMA (5:5) hydrogel is the most promising one for nerve tissue engineering applications in terms porosity, pore size, mechanical strength, SC attachment and proliferation. PC12 cells were attached and proliferated on

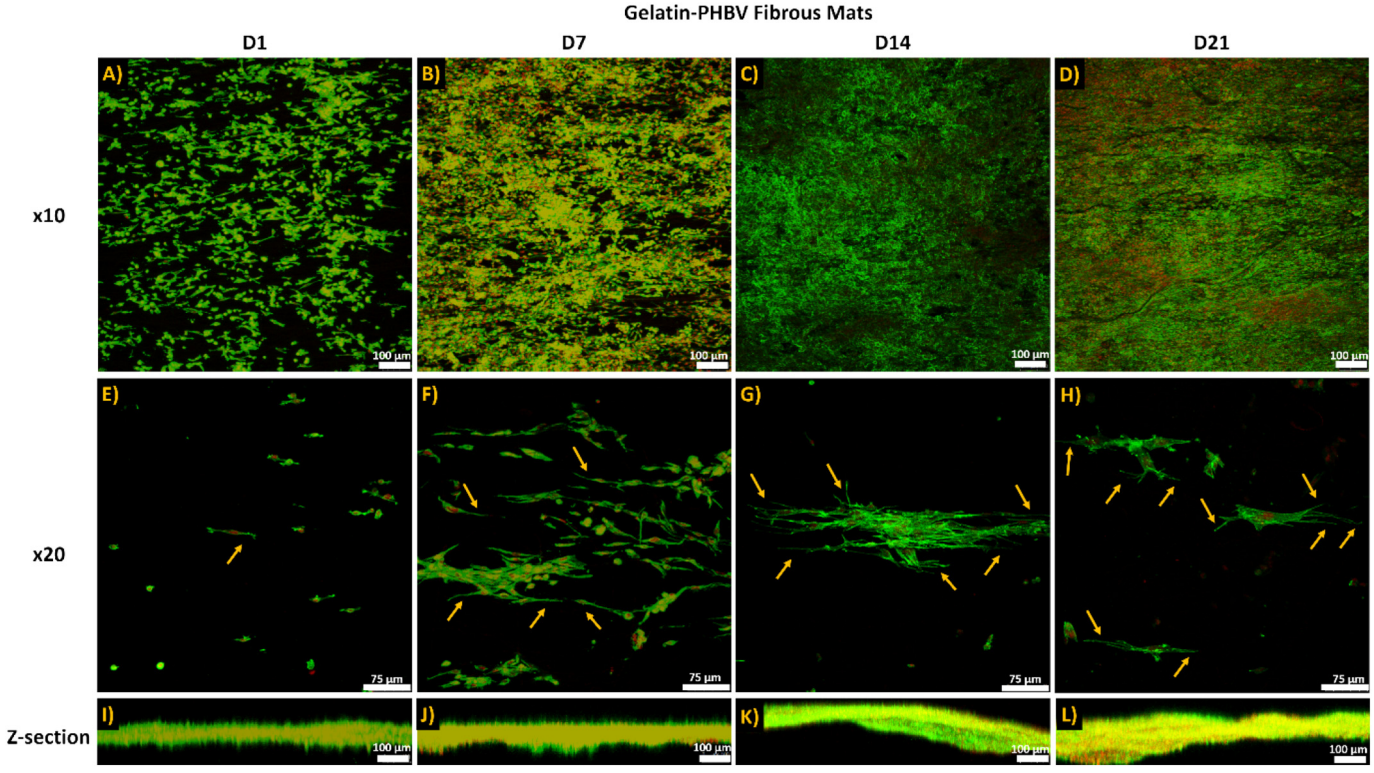

Fig. 7. Cytoskeleton (green) and nucleus (red) merged CLSM images of PC12 cells on gelatin-PHBV aligned fibrous mats. A) Day 1, 10×, B) Day 7, 10×, C) Day 14, 10×, D) Day 21, 10×, E) Day 1, 20×, F) Day 7, 20×, G) Day 14, 20×, H) Day 21, 20×, I) Day 1, z-section, J) Day 7, z-section, K) Day 14, z-section, L) Day 21, z-section. Arrows show the neurite outgrowth.

gelatin-PHBV (5:5) aligned fibrous mats, and cells aligned themselves along the fibers. Therefore, combination of GelMA-pHEMA (5:5) hydrogel and gelatin-PHBV aligned fibrous mat would serve as an ideal nerve guide. As future studies, both Schwann and PC12 cells grown on the scaffolds will be characterized by staining with cell-specific markers such as beta tubulin, Neu N and myelin basic protein (MBP).

Acknowledgments

We acknowledge the support by METU (BAP 07.02.2012-101) and METU CoE in Biomaterials and Tissue Engineering (BIOMATEN). We also gratefully acknowledge the Ministry of Development of Turkey (BAP 01.08.DPT.2003K120920-20) and the Scientific and Technological Research Council of Turkey (2205 BIDEP-TUBITAK Fellowship for TDU).

References

[1] R.M.G. Menorca, T.S. Fussell, J.C. Elfar, Nerve physiology: mechanisms of injury and recovery, Hand Clin. 29 (2013) 317–330.
[2] D. Arslantunali, T. Dursun, D. Yucel, N. Hasirci, V. Hasirci, Peripheral nerve conduits: technology update, Med. Devices Evid. Res. 7 (2014) 405–424.
[3] X. Gu, F. Ding, D.F. Williams, Neural tissue engineering options for peripheral nerve regeneration, Biomaterials 35 (2014) 6143–6156.
[4] D. Grinsell, C.P. Keating, Peripheral nerve reconstruction after injury: a review of clinical and experimental therapies, Biomed. Res. Int. 698256 (2014).
[5] S. Mobini, B.S. Spearman, C.S. Lacko, C.E. Schmidt, Recent advances in strategies for peripheral nerve tissue engineering, Curr. Opin. Biomed. Eng. 4 (2017) 134–142.
[6] S.A. Zadegan, M. Firouzi, M.H. Nabian, L.O. Zanjani, R.S. Kamrani, Two-stage nerve graft using a silicone tube, Front. Surg. 2 (2015) 12.
[7] D. Arslantunali, G. Budak, V. Hasirci, Multiwalled CNT-pHEMA composite conduit for peripheral nerve repair, J. Biomed. Mater. Res. A 102 (2014) 828–841.
[8] J.H.A. Bell, J.W. Haycock, Next generation nerve guides: materials, fabrication, growth factors, and cell delivery, Tissue Eng. Part B Rev. 18 (2012) 116–128.
[9] L. Yan, et al., Aligned nanofibers from polypyrrole/graphene as electrodes for regeneration of optic nerve via electrical stimulation, ACS Appl. Mater. Interfaces 8 (2016) 6834–6840.
[10] S.G.A. van Neerven, et al., Two-component collagen nerve guides support axonal regeneration in the rat peripheral nerve injury model, J. Tissue Eng. Regen. Med. 11 (2017) 3349–3361.
[11] J. Tao, et al., A 3D-engineered porous conduit for peripheral nerve repair, Sci. Rep. 7 (2017) 46038.
[12] Q. Guo, et al., Chitosan conduits filled with simvastatin/Pluronic F-127 hydrogel promote peripheral nerve regeneration in rats, J Biomed Mater Res B Appl Biomater 106 (2) (2018) 787–799.
[13] I. Ortuño-Lizarán, G. Vilariño-Feltrer, C. Martínez-Ramos, M.M. Pradas, A. Vallés-Lluch, Influence of synthesis parameters on hyaluronic acid hydrogels intended as nerve conduits, Biofabrication 8 (2016), 045011.
[14] A.M. Ghaznavi, L.E. Kokai, M.L. Lovett, D.L. Kaplan, K.G. Marra, Silk fibroin conduits: a cellular and functional assessment of peripheral nerve repair, Ann. Plast. Surg. 66 (2011) 273–279.
[15] A.R. Nectow, K.G. Marra, D.L. Kaplan, Biomaterials for the development of peripheral nerve guidance conduits, Tissue Eng. Part B Rev. 18 (2012) 40–50.
[16] V. Miguez-Pacheco, L.L. Hench, A.R. Boccaccini, Bioactive glasses beyond bone and teeth: emerging applications in contact with soft tissues, Acta Biomater. 13 (2015) 1–15.
[17] G.H. Borschel, K.F. Kia, W.M. Kuzon, R.G. Dennis, Mechanical properties of acellular peripheral nerve, J. Surg. Res. 114 (2003) 133–139.
[18] K.R. Jessen, R. Mirsky, The repair Schwann cell and its function in regenerating nerves, J. Physiol. 594 (2016) 3521–3531.
[19] C. Meyer, et al., Peripheral nerve regeneration through hydrogel-enriched chitosan conduits containing engineered Schwann cells for drug delivery, Cell Transplant. 25 (2016) 159–182.
[20] Y. Wu, L. Wang, B. Guo, Y. Shao, P.X. Ma, Electroactive biodegradable polyurethane significantly enhanced Schwann cells myelin gene expression and neurotrophin secretion for peripheral nerve tissue engineering, Biomaterials 87 (2016) 18–31.
[21] A.D. Levi, S.S. Burks, K.D. Anderson, M. Dididze, A. Khan, W.D. Dietrich, The use of autologous Schwann cells to supplement sciatic nerve repair with a large gap: first in human experience, Cell Transplant. 25 (2016) 1395–1403.
[22] C.J. Pateman, et al., Nerve guides manufactured from photocurable polymers to aid peripheral nerve repair, Biomaterials 49 (2015) 77–89.
[23] Y.-S. Lee, T. Livingston Arinzeh, Electrospun nanofibrous materials for neural tissue engineering, Polymers (Basel, Switz.) 3 (2011) 413–426.
[24] C.M.A.P. Schuh, et al., Activated Schwann cell-like cells on aligned fibrin-poly(lactic-co-glycolic acid) structures: a novel construct for application in peripheral nerve regeneration, Cells Tissues Organs 200 (2015) 287–299.
[25] C.J. Pateman, et al., Biomaterials nerve guides manufactured from photocurable polymers to aid peripheral nerve repair, Biomaterials 49 (2015) 77–89.
[26] S.-J. Lee, M. Nowicki, B. Harris, L.G. Zhang, Fabrication of a highly aligned neural scaffold via a table top stereolithography 3D printing and electrospinning, Tissue Eng. Part A 23 (2017) 491–502.
[27] T. Dursun Usal, D. Yucel, V. Hasirci, Differentiation of BMSCs into nerve precursor cells on Fiber-foam constructs for peripheral nerve tissue engineering, J. Sib. Fed. Univ. 11 (2018) 119–130.
[28] W. Meng, et al., Synthesis of gelatin-containing PHBV nanofiber mats for biomedical application, J. Mater. Sci. Mater. Med. 19 (2008) 2799–2807.
[29] J.W. Nichol, S.T. Koshy, H. Bae, C.M. Hwang, S. Yamanlar, A. Khademhosseini, Cell-laden microengineered gelatin methacrylate hydrogels, Biomaterials 31 (2010) 5536–5544.
[30] D. Yucel, G.T. Kose, V. Hasirci, Polyester based nerve guidance conduit design, Biomaterials 31 (2010) 1596–1603.
[31] J. O'Brien, I. Wilson, T. Orton, F. Pognan, Investigation of the Alamar Blue (resazurin) fluorescent dye for the assessment of mammalian cell cytotoxicity, Eur. J. Biochem. 267 (2000) 5421–5426.
[32] W.T. Brinkman, K. Nagapudi, B.S. Thomas, E.L. Chaikof, Photo-cross-linking of type I collagen gels in the presence of smooth muscle cells: mechanical properties, cell viability, and function, Biomacromolecules 4 (2003) 890–895.
[33] X. Li, et al., Thermosensitive N-isopropylacrylamide–N–propylacrylamide-vinyl pyrrolidone terpolymers: synthesis, characterization and preliminary application as embolic agents, Biomaterials 26 (2005) 7002–7011.
[34] Gianluca Ciardelli, et al., Blends of poly-(ε-caprolactone) and polysaccharides in tissue engineering applications, Biomacromolecules 6 (2005) 1961–1976.
[35] J.F. Almeida, P. Ferreira, A. Lopes, M.H. Gil, Photocrosslinkable biodegradable responsive hydrogels as drug delivery systems, Int. J. Biol. Macromol. 49 (2011) 948–954.
[36] Q.L. Loh, C. Choong, Three-dimensional scaffolds for tissue engineering applications: role of porosity and pore size, Tissue Eng. Part B Rev. 19 (2013) 485–502.
[37] V. Salih, Biodegradable scaffolds for tissue engineering, in: L.D. Silvio (Ed.), Cellular Response to Biomaterials, Woodhead Publishing, Cambridge 2009, pp. 185–211.
[38] C. Frantz, K.M. Stewart, V.M. Weaver, The extracellular matrix at a glance, J. Cell Sci. 123 (2010) 4195–4200.
[39] A.S. Badami, M.R. Kreke, M.S. Thompson, J.S. Riffle, A.S. Goldstein, Effect of fiber diameter on spreading, proliferation, and differentiation of osteoblastic cells on electrospun poly(lactic acid) substrates, Biomaterials 27 (2006) 596–606.